105 (2026) 106581

Contents lists available at ScienceDirect

Poultry Science

journal homepage: www.elsevier.com/locate/psj

Full-Length Article

Insights into speckled eggs provided by single-cell transcriptomics in high-yield laying hens

Yan Sun [a,b,d], Jing Zhang [a,b,c,d,e], Zhongsheng Chen [a,b,d], Wei Liu [a,b,d], Haixia Han [a,b,d], Dan Hao [a,b,d], Dapeng Li [a,b,d], Jie Wang [a,b,d], Jie Liu [a,b,d], Qiuxia Lei [a,b,d], Yan Zhou [a,b,d], Dingguo Cao [a,b,d], YunChao Wang [c], Guiming Li [a,b,c,d], Fu Chen [e], Fuwei Li [a,b,c,d,*]

[a] Poultry Institute, Shandong Academy of Agricultural Sciences, 250100, Jinan, China
[b] Shandong Provincial Key Laboratory of Livestock and Poultry Breeding (PKL2024B15), Jinan, 250023, Shandong, China
[c] Shandong Blue Horizon Ecological Agriculture Co., Ltd, 257094, Dongying, China
[d] Jinan Key Laboratory of Poultry Germplasm Resources Innovation and Healthy Breeding, Jinan, 250100, China
[e] College of Veterinary Medicine, Qingdao Agricultural University, Qingdao, 266109, China

ARTICLE INFO

Key words:
Speckled eggs
scRNA-seq
Uterus
Eggshell quality
Chicken

ABSTRACT

Eggshell quality is a major concern in the poultry industry. The speckle phenotype in eggshell affects eggshell color, thickness, and Haugh Unit (**HU**) and significantly affects the hatchability rate. The rate of speckled eggs increases during the late-laying period, which can lead to notable economic losses. Eggshell speckles have medium heritability; however, the genetic architecture of speckled eggshells remains unclear. In this study, the chickens were divided into two groups based on the rate of egg speckling. Uterine tissues were collected and analyzed using 10X Genomics single-cell RNA sequencing to delineate the molecular signatures of the various cell types. A total of 10 cell types were identified: immune (B, T, monocyte macrophages, and plasma cells), endothelial, epithelial, stromal, neuroendocrine, serous, and protoporphyrin IX pigment cells. The trends of cell type distributions were consistent in two groups. Functional enrichment analysis showed that unique biological processes, such as IgA production and Toll-like C-type lectin receptor signaling pathways, were enriched in immune cells, whereas TGF-beta, Wnt, and NOD-like receptor signaling pathways were enriched in epithelial cells. Subsequently, we identified differentially expressed genes in the two groups, among which *SPP1* (secreted phosphoprotein 1) was down-regulated in all cell types in the speckled group. The cellular interaction signals of speckled group were significantly enhanced compared to the control group. The cell proliferation and differentiation pathways mediated by WNT, SPP1, and BMP were inhibited and the interaction related to cell migration was activated in the speckled group. This study explored cell heterogeneity, extended prior findings by adding single-cell resolution atlas, and identified cell type specific patterns that can guide future functional studies of speckled eggs.

Introduction

Eggs are an important and economical source of animal protein. Egg quality parameters, including albumen height, Haugh Unit (**HU**), egg yolk ratio, and yolk color, reflect the nutritional value and freshness of eggs. In addition, eggshell traits, including eggshell color, shape index, strength, thickness, translucency, and speckles, are related to resistance to microbial invasion (Sirri et al., 2018) and significantly influence consumer preferences. Speckles are irregular reddish-brown marks on the surface of the eggshells. The appearance of spots is a manifestation of uneven eggshell pigment deposition and is widely observed in brown-shelled eggs, particularly those laid by older laying hens.

In recent years, the trend of extended laying cycles has become increasingly significant. However, an extended laying cycle is associated with a decline in eggshell quality, resulting in a light eggshell color, increased eggshell weight, and speckled eggshells (Molnar et al., 2016).

* Corresponding author.
E-mail address: lifuwei1224@163.com (F. Li).

https://doi.org/10.1016/j.psj.2026.106581
Received 8 August 2025; Accepted 1 February 2026
Available online 2 February 2026

Speckle traits affect eggshell color, thickness, and HUs, resulting in decreased egg freshness.

Previous research have pointed that age, light intensity, dietary nutrients, environmental changes (such as oxidative stress) and genetic information can affect the formation of speckled eggs (Cheng et al., 2019; Lewis et al., 2008). The hatchability rate of speckled eggs is significantly lower than that of normal eggs ($P < 0.05$), resulting in considerable economic losses (Cheng et al., 2023c; Duan, et al., 2023). Therefore, reducing the incidence of speckled eggs and analyzing the genetic mechanisms underlying speckle trait formation are necessary.

Eggshell speckles are a moderately heritable trait (0.22−0.38) and are related to extreme selection for eggshell color during breeding (Arango et al., 2006; Cheng et al., 2023b). A genome-wide association study (**GWAS**) of the eggshell speckle phenotype in purebred Rhode Island was conducted to detect potential genomic loci and candidate genes, including 311 single nucleotide polymorphisms (**SNPs**) (six significantly and 305 suggestively associated) and 39 candidate genes. Pathway analysis revealed alpha-linolenic acid metabolism, linoleic acid metabolism, ether lipid metabolism, GnRH signaling pathway, vascular smooth muscle contraction, and MAPK signaling pathways (Cheng et al., 2023b). The uterus (eggshell gland) forms the complete eggshell structure, outer cuticle, and pigmentation (Samiullah et al., 2015; Wilson et al., 2017). Integrative transcriptome and methylome data analysis of the uterine mucosa identified *BFSP2* as a key gene involved in this process, which was expressed at low levels and hypomethylated in the speckled group (Cheng et al., 2023a). Duan et al. (2023) conducted histological observations and transcriptome analyses of the uterine tissue of laying hens that produced normal and speckled eggs. The lower the cilia density, the more the epithelial cells tend to defect with poor integrity in the speckled group, and the biological processes of differentially expressed genes were mainly involved in the immunological function and embryonic growth of chickens. However, further functional verification of the identified genes is required.

The ultrastructure of speckled eggshells has also been reported, suggesting that the eggshell in the speckled region is thick, with loose material between the vertical crystal and cuticle layers. Moreover, the protoporphyrin IX content in the speckled region was significantly higher than that in the adjacent normal region ($P < 0.01$) (Cheng et al., 2023c). Underwood and Sealy (2002) reported that the primary constituent of eggshell speckles is protoporphyrin IX. These results suggest that the synthesis and deposition of protoporphyrin IX are closely related to speckle formation. However, the genetic mechanisms underlying the formation of eggshell speckles remain unclear.

In farm animals, single-cell RNA sequencing (scRNA-seq) has been widely used to determine the expression profiles of different tissues during development, physiology, and disease (Potter, 2018; Wang et al., 2022). Thousands of single cells from a single tissue can be analyzed using unique molecular identifiers (**UMI**) to reveal cellular signatures and cell communication (Trapnell, 2015). In addition, scRNA-seq technology can be used to explore different cellular functions and developmental trajectories in human and animal models (Garcia-Alonso et al., 2022; Xu et al., 2023; Zhao et al., 2022). Rao et al. (2023) presented the most comprehensive postnatal liver development single-cell atlas and demonstrated metabolic and immune changes across four age stages. In studies related to reproductive traits, single-cell transcriptome analysis of male chicken germ cells revealed that the transcriptional levels of components of the MAPK, Hedgehog, and thyroid hormone signaling pathways were steadily upregulated after mitotic arrest, suggesting the cooperation of multiple signaling pathways during entry into mitotic arrest and the subsequent quiescence of male chicken germ cells (Choi et al., 2023). Estermann et al. (2020) performed a comprehensive analysis of the gonads of embryonic chickens during sexual differentiation using scRNA-seq to study the gonadal sex differentiation process. Wang et al. (2024) analyzed two sides of the ovaries at six distinct embryonic developmental stages using single-cell transcriptome sequencing and provided insights into the left-right asymmetric development of the chicken ovary, particularly the role of cortex cells in the left ovary. scRNA-seq has revealed the molecular regulatory mechanisms of sheep spermatogenesis and highlighted gene conservation during spermatogenesis in sheep and humans (Tian et al., 2022). Single-cell sequencing has revealed reproductive variations between primiparous and multiparous Hu ewes, providing insights into the molecular mechanisms underlying the high fecundity of Hu sheep (Ge et al., 2023). Xu et al. (2023) revealed a comprehensive age-associated transcriptomic atlas using ovarian data at different stages at the single-cell level and identified new diagnostic biomarkers and potential therapeutic targets for age-related ovarian diseases. Li et al. (2020) compared the single-cell transcriptome data of chicken breast muscle at two developmental stages, identified cell clusters, captured the gene expression of single cells, and identified two genes, *APOA1* and *COL1A1*, as biomarkers of intramuscular fat cells. In terms of chicken peripheral blood leukocytes, in addition to major leukocyte cells, a new subpopulation of chicken peripheral B-cells with high *SOX5* expression was identified, along with TCRγ/δ + *T*-cell subpopulations including at least two subtypes (Maxwell et al., 2024). Zhang et al. (2024) explored the regulative mechanisms of follicular selection and atresia in chicken granulosa cells using single-cell RNA sequencing.

GWAS of eggshell quality traits and proteomic research in uterine fluid were performed to identified key genes and proteins of eggshell (Chen et al., 2024; Gao et al., 2025). Despite previous studies on uterus of egg-laying hens, no study has explored the chicken oviduct, particularly the uterus, using single-cell RNA sequencing. Considering the critical role of the chicken oviduct in egg formation as the yolk travels through the infundibulum, magnum, and isthmus and reaches the uterus, a single-cell perspective could uncover new regulatory mechanisms of speckle formation. In this study, a single-cell transcriptome using 10X Genomics Cr was used to elucidate the diversity of the cell profiles in the chicken uterus. Typical cell-specific genes were verified using RNA in situ hybridization. Our aim was to address the existing gap in the single-cell characterization of the uterus and provide new insights into the genetic and cellular basis of speckled eggshell formation.

Materials and methods

Chicken management

Thirty Hy-Line brown laying hens (72 weeks old) were raised in individual cages under the same routine conditions of nutrition, vaccination, and management. A laying hen lighting program was adopted during the experimental period. Mashed feed and fresh water were provided, ad libitum. After observing and determining the probability of producing speckled eggs for more than seven days, the chickens were divided into two groups: control and speckled.

Uterine tissue collection and dissociation

Six hens (three in the control group [C1, C2, C3] and three in the speckled egg group [S1, S2, S3]) were euthanized after oviposition, and the uterus was isolated, rinsed with phosphate-buffered saline (**PBS**), and cut into pieces. Part of the uterine tissue was fixed in 4% formaldehyde for RNA in situ hybridization, and the other part was used to detect protoporphyrin IX content. Other uterine samples from the same position were stored in MASC tissue storage solution (cat#130-100-008, Miltenyi Biotec, USA) and immediately transferred to the laboratory for single-cell dissociation within 24 h.

Uterine tissues were dissociated into single cells in dissociation solution in a 37°C water bath with shaking for 20 min at 100 rpm. Digestion was terminated using 1 × PBS containing 10% fetal bovine serum (**FBS**). The cell suspension was filtered and centrifuged at 300 × *g* for 5 min at 4°C. The cell pellets were resuspended and incubated at room temperature. After incubation, the cell debris and dead cells were removed. The overall cell viability reached > 85%, and the

concentration of single-cell suspensions was adjusted to 700–1200 cells/μL for the 10X Genomics Chromium™ system.

scRNA-seq data processing and analysis

Single-cell mRNA libraries were generated using the Single-Cell 3′ Reagent V3 Kit (10X Genomics, Pleasanton, CA, USA) according to the manufacturer's protocol. cDNA libraries were amplified by PCR using 15 cycles. Libraries were sequenced on an Illumina NovaSeq 6000 (Illumina, San Diego, CA, USA) by LC-Bio Technology Co. Ltd. (Hangzhou, China) at a minimum depth of 20,000 reads per cell.

After sequencing, Cell Ranger software (version 7.2.0) was used to perform preliminary processing, and the FASTQ files were mapped to the chicken genome reference (https://ftp.ensembl.org/pub/release-110/fasta/gallus_gallus/cdna/Gallus_gallus.bGalGal1.mat.broiler.GRCg7b.cdna.all.fa.gz). The R package Seurat (version 4.1.1) was used for dimensional reduction and clustering (Butler et al., 2018). The control threshold was set as follows: all genes expressed in less than three cells, the number of genes expressed per cell was over 500, and the percent of mitochondrial genes was less than 25%. The LogNormalize method was used to normalize expression levels, The clustering algorithm optimized based on the shared nearest neighbor (SNN) module for identifying cell clusters, while using harmony to remove batch effects. The cells were then visualized in two dimensions using Uniform Manifold Approximation and Projection (**UMAP**). We set the random seed to 10086, the resolution to 0.8, and select dims as 20 to complete dimensionality reduction clustering. Single-cell data analysis was performed using the OmicStudio tools created by LC-BIO Co., Ltd (HangZhou, China) at https://www.omicstudio.cn/cell.

Cell type annotation and difference analysis

We artificially annotated the clusters into different cell types based on a cell marker dataset. The cell-type proportions between groups were performed using t-test. Specifically, we identified the marker genes and differentially expressed genes (**DEGs**) of each cell-type using the 'bimod' test as implemented in the Seurat FindMarkers function, $P < 0.01$, $\log_2$ (Fold Change) > 0.26, the minimum % expression cutoffs threshold was set 0, and markers genes which were expressed in more than 10% of the cells in a cluster (Mcdavid et al., 2013). The bimod algorithm, which can precise identification of genes featuring subpopulation-specific expression, and allow for unsupervised screening of core markers that drive cellular heterogeneity from a vast pool of genes. Gene Ontology (**GO**) enrichment and Kyoto Encyclopedia of Genes and Genomes (**KEGG**) pathway enrichment analyses of DEGs were performed using R, indicating a $P \leq 0.05$ for significant gene enrichment.

Marker gene verification by RNA in situ hybridization

Uterine tissue was fixed overnight in 4% paraformaldehyde at 4°C. The samples were then embedded in paraffin. The sections were used for in situ RNA hybridization. Probes for three genes (*KRT18, PIGR*, and *CLDN10)* were designed. *KRT18* was used as the positive control. The uterine sections were pretreated with protease K. The pretreated sections were hybridized with RNA probes in a hybridization solution overnight. After RNA in situ hybridization, the nuclei were counterstained with DAPI for 8 min at room temperature. A fluorescent microscope (Zeiss, Axo Observer 3, Germany) and CaseViewer 2.4.0 (3DHistech, Budapest, Hungary) were used for imaging. The three probes were located in different probe channels and labeled with different fluorescence tags using TSA Plus fluorophore.

Cell communication analysis

Signaling crosstalk is critical for informing diverse cellular decisions, such as the activation of the cell cycle, cell death, migration, and differentiation (Giladi et al., 2020). To elucidate cell-cell communication within the uterine tissue, a comprehensive analysis of signaling crosstalk was conducted using the Python package CellPhoneDB (v5.0.0). The top 20 significant ligand-receptor interactions were generated using the R package ggplot2 (version 3.3.0).

Results

Comparison of speckled ratio and detection protoporphyrin IX

After evaluating the eggshell phenotype for two weeks, six chickens were selected and grouped. The results showed that the ratio of speckled egg production was > 75% in the speckled group (Table 1). Protoporphyrin IX content in the uterine tissues of the two groups was detected using ELISA test kits. As shown in Table 2, the protoporphyrin IX content in the uterine tissue of the speckled group was significantly higher than that of the control group ($P < 0.05$).

Chicken uterine cell types profiling using single-cell transcriptome

In total, 49,755 single cells were captured from the two groups (27,500 and 22, 255 cells in the control and speckled egg groups, respectively). Overall, 33,815 cells passed quality control after critical cell filtration (Supplementary Table 1). The number of cells obtained from each sample ranged from 3,045 to 6,832. The average number of genes in each cell ranged from 2,160 to 3,003.

Based on the sequencing data, 25 clusters were identified using UMAP analysis. We characterized the cell types using existing cell markers provided by the reference, Fig. 1A and 1B respectively presented the 10 major cell atlas of the two groups. Distinct expression patterns of the selected signature genes for each cell type were visualized using a dot matrix (Fig. 1C). Stromal cells were identified with high expression levels of marker genes, including *PDGFRA, DCN*, and *TCF21*. Epithelial cells were identified based on the expression of *PIGR, CLDN10* and *EDIL3*. Using marker genes including *PSCA, ALAS1, RARRES1*, and *SPINK5*, we identified protoporphyrin IX-synthesized cells. T lymphocytes were annotated based on the expression levels of *CD3D*, and *CD3E*. Monocyte/macrophage cell was specifically expressed at high levels of the marker genes, *LYZ, CD14*, and *MARCO*. Cells were annotated as neuroendocrine cells based on *CHGB* and *SCG2* expression. Furthermore, other important cell types were identified, including endothelial cells (*EMCN, VWF*, and *CDH5*), serous cells (*CA2* and *SPP1*), plasma cells (*JCHAIN* and *MZB1*). The distribution of cell types was presented in each samples (Fig. 1D). There was no significant difference in the proportion of cell types between two groups using T-test. The serous and stromal cells were the main cell types in the control group, B cells and T cells were also account for high proportions in the speckled group (Supplementary Table 2). Two marker genes were selected and verified using RNA in situ hybridization. The expression patterns of *PIGR* and *CLDN10* in uterine tissues were similar to those of *KRT18*. The fluorescence results confirmed the expression and localization in the cell types (Fig. 2).

Gene expression signatures in cell types

The upregulated genes in each cell type were identified (Supplementary Table 3). Most genes are specifically expressed in their respective cell types. Fig. 3 shows marker genes for cell types and GO and KEGG enrichment data revealed typical cellular functions. Metabolic and oxidative phosphorylation pathways were significantly

Table 1
Comparison of the speckled eggs ratio between two groups.

	Control Group			Speckled Group		
Samples	C1	C2	C3	S1	S2	S3
Speckled rate (%)	0	0	0	75	83	75

Table 2
Content of protoporphyrin IX in uterus.

Items	Control Group	Speckled Group	*P* Value
Content (ng/mL)	46.26±5.47[b]	52.66±5.95[a]	0.02

a,b Values differ significantly at $P < 0.05$.

enriched in endothelial, epithelial, neuroendocrine, serous, and protoporphyrin IX-synthesizing cells. The key marker genes of immune cells annotated representative pathways, including IgA production, Toll-like receptor signaling, and C-type lectin receptor signaling pathways. MAPK, focal adhesion, and forkhead box O (FoXo) signaling pathways were enriched in endothelial cells. TGF-beta signaling pathway, WNT signaling pathway, and NOD-like receptor signaling pathway were enriched in epithelial cell.

Differential cell expression profiles between two groups

Fig. 4 shows differential expression between control and speckled groups. Most DEGs were identified in the stromal and serous cells

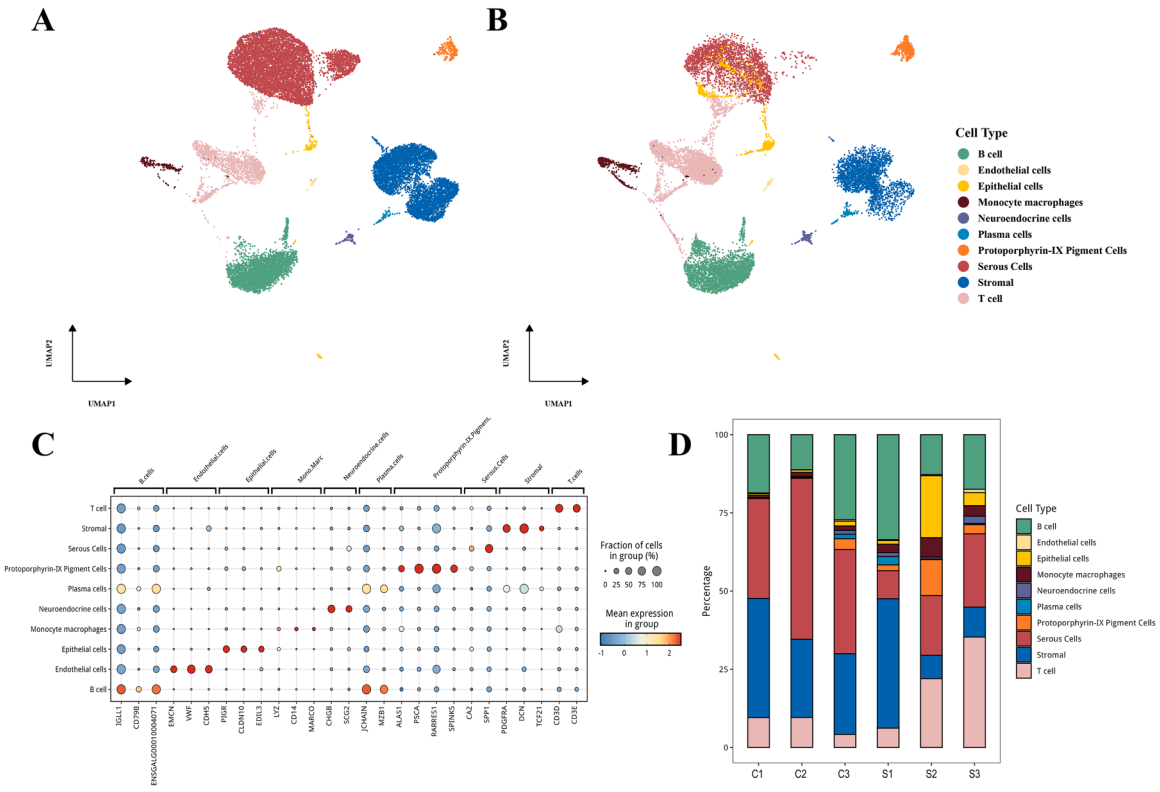

Fig. 1. Identification of chicken uterine cell types by single-cell RNA-seq transcriptomics. **A** UMAP plot of ten cell types in control group. Each point represents an cell. **B** Identification ten cell types on UMAP in speckled group. **C** Dot plot of different cell marker gene expression levels. **D** Bar plot showing the proportion of cell types in two groups.

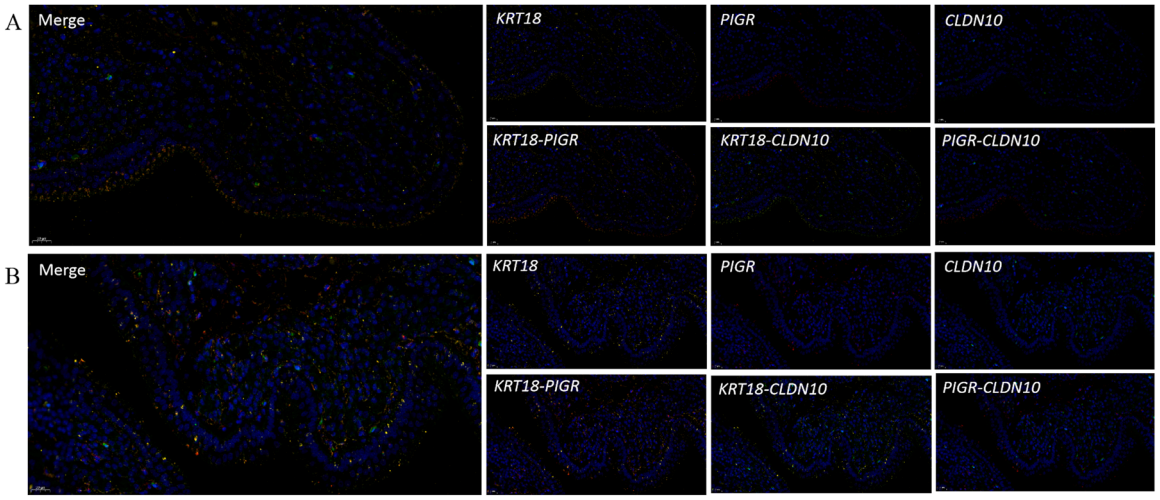

Fig. 2. In situ validation of mRNA expression of the marker genes *KRT18, PIGR*, and *CLDN10* in uterine tissue. *PIGR*, and *CLDN10* are selected from up-regulated genes in epithelia cell, *KRT18* is a known marker gene and used as a positive control. **A** The expression and localization in control group. **B** presents the results of speckled group.

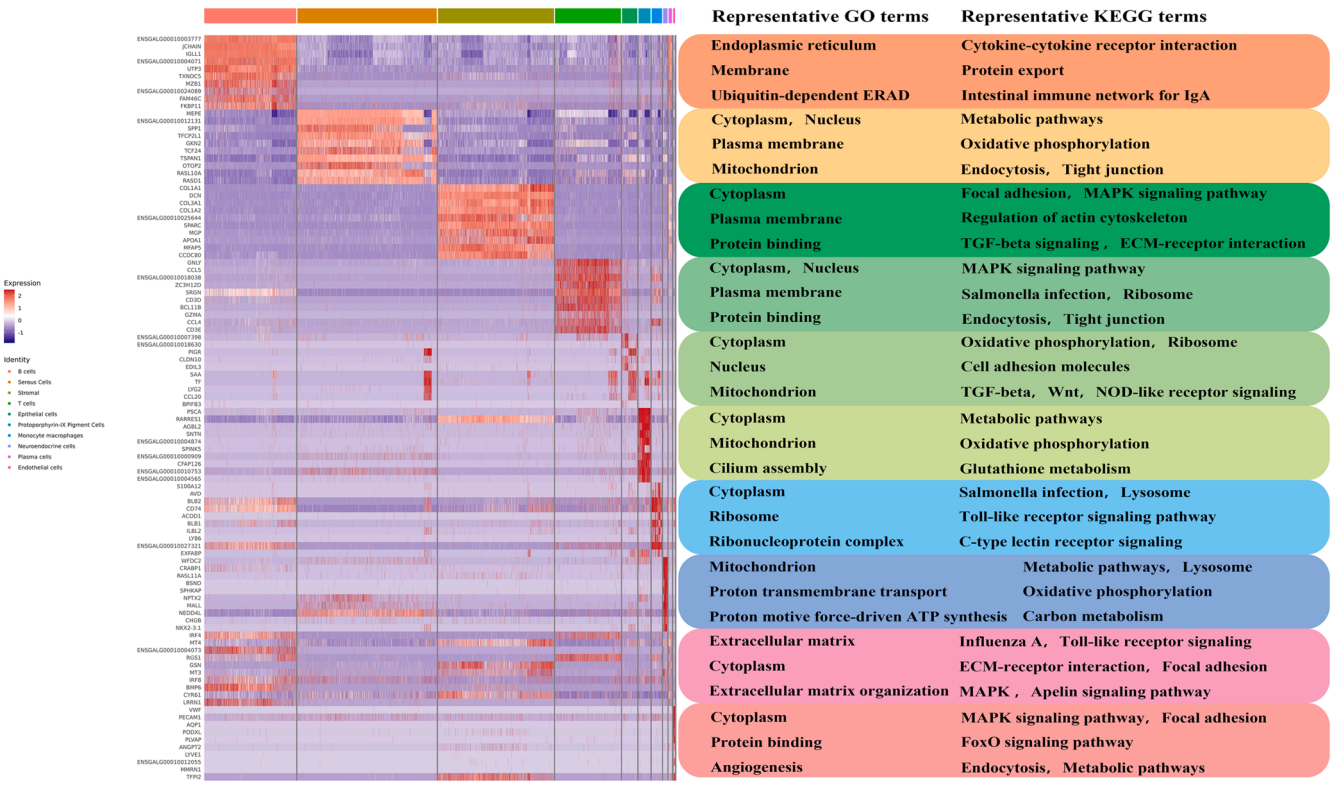

Fig. 3. The marker genes of cell types and function enrichment.

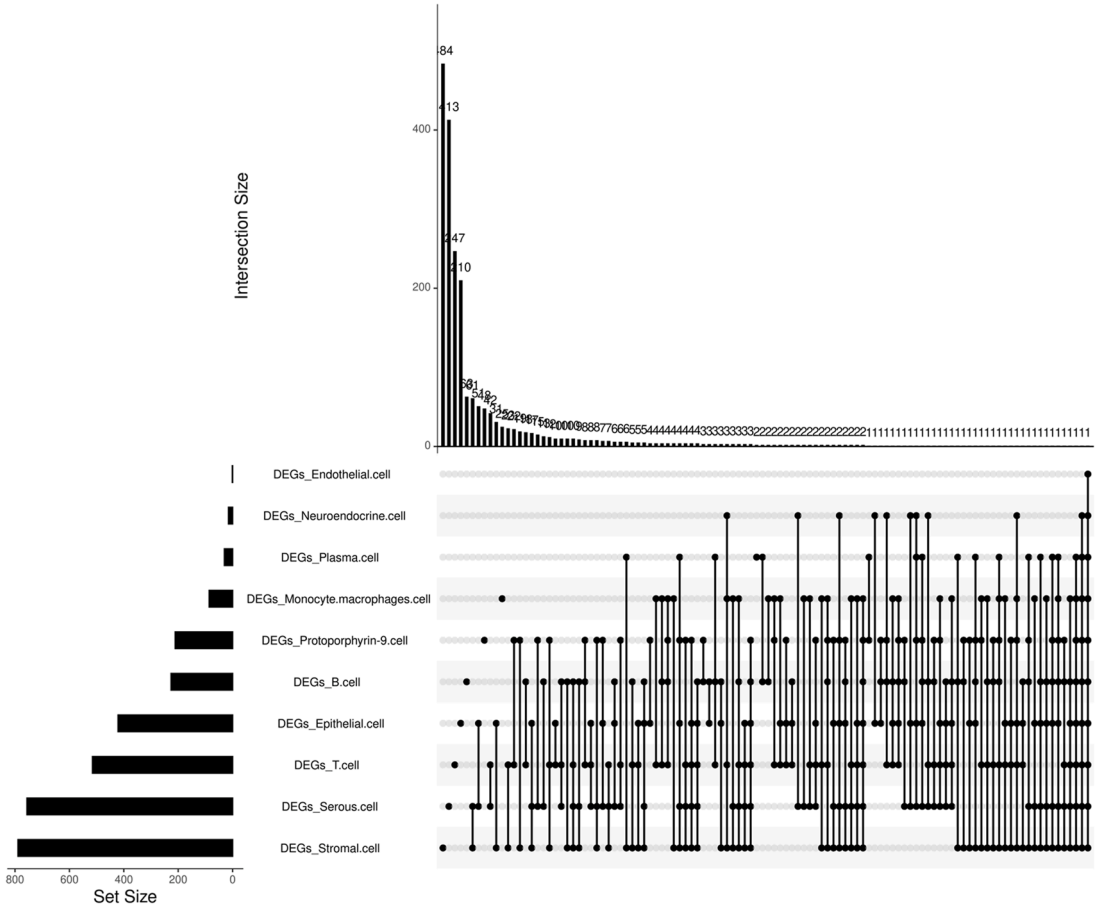

Fig. 4. Differential expression between control and speckled groups.

(Supplementary Table 4). A total of 560 upregulated and 229 downregulated DEGs were identified in stromal cells, 307 upregulated and 449 downregulated DEGs in serous cells, 310 upregulated and 111 downregulated DEGs were identified in epithelial cells, 123 upregulated and 88 downregulated DEGs in protoporphyrin IX-synthesizing cells, and six upregulated and nine downregulated DEGs in neuroendocrine cells. Only one DEG, *SPP1* (secreted phosphoprotein 1), was found in endothelial cells, and a total of 593 upregulated DEGs and 1020 downregulated DEGs were identified in immune cells. Notably, *SPP1* expression was down-regulated in all cell types in the speckled group. Excluding endothelial cells, the other nine cell types intersected with one gene- the matrix extracellular phosphoglycoprotein (*MEPE*), which was down-regulated in the speckled group. *SPP1* was verified using RNA in situ hybridization in both groups. As shown in Fig. 5, the fluorescence signal of *SPP1* in the control group was significantly stronger than that in the speckled group.

To shed further light on the putative functions of the DEGs, KEGG enrichment analyses were conducted with the identified DEGs (Supplementary Table 5). In stromal cells, the DEGs were significantly enriched in the ribosome, focal adhesion, TGF-beta signaling pathway, and regulation of actin cytoskeleton. In serous cells, the enriched signaling pathways included metabolic pathways, phagosomes, C-type lectin receptor signaling pathways, NOD-like receptor signaling pathways, and TGF-β signaling pathways. The enriched pathways of DEGs in epithelial cells were mainly related to metabolic pathways, Salmonella infection, phagosomes, and cell adhesion molecules. The DEGs in protoporphyrin IX-synthesized cells were enriched for oxidative phosphorylation and focal adhesion. Significantly enriched pathways in immune cells included apoptosis, *Salmonella* infection, ECM-receptor interactions, and the immune network for IgA production.

Signaling crosstalk among various cell types

A cell-to-cell communication network was constructed based on ligands and matching receptors expression information from our single-cell atlas (Fig. 6A). The key cellular interactions have been identified, including serous cells, protoporphyrin_IX pigment cells, epithelial cells and neuroendocrine cells. Fig. 6B and Fig. 6C displayed the interacted strength between cells in two groups, separately. The result showed the interaction signals of speckled group were significantly enhanced compared to the control group. Further exploration was conducted on the abundance of ligand-receptor interactions (Fig. 6D and Fig. 6E). Conserved interaction signals were detected in two groups, stromal cells were predicted to communicate with endothelial cells and serous cells through COL4A1-integrin a11b1 complex and COL4A1-integrin a1b1 complex interactions in the control group. COL4A1-integrin communication was related to cell adhesion, the signal abundance of these ligand-receptor suggested the communication intensity related to cell adhesion is significantly weakened in the speckled group. In cell transduction, APP-SORL1, APP-TNFRSF21, and APP-CD74 interactions were detected in multiple cell pairs of two groups. However, APP-CD74 has a stronger signal in cell pairs such as stromal cells to epithelial cells and endothelial cells to protoporphyrin IX pigment-synthesizing cells in speckled group, indicating cellular transduction mediated by this signal is upregulated in the speckled group.

There were also significantly altered interaction signals, reflecting the activation/inhibition of specific signaling pathways. WNT5A-FRZB, SPP1-integrin αVβ3 complex, and BMP6 related interactions were unique detected in control group. These ligand-receptor showed no significant signals in speckled group, suggesting the cell proliferation and differentiation pathways mediated by WNT, SPP1, and BMP were inhibited in the speckled group. However, EFNB1-EPHB1, JAG1-NOTCH1, and CXCL12-CXCR4 pairs were only appeared in speckled group, which suggested the interaction network related to cell differentiation and migration was activated in the speckled group.

Discussion

The heritability of eggshell speckles was 0.35 at 28 weeks of age (Cheng et al., 2023b). The formation of speckles has a significant effect on eggshell color, and the L-, a-, and b-values are significantly different from those in normal egg groups (Duan et al., 2023). The uterus is an important organ that forms the eggshell. Therefore, the transcriptional profiles of the uterus are essential for investigating the mechanisms underlying speckled traits on the eggshell surface. In the present study, we investigated the differences in the expression profiles of the uterus

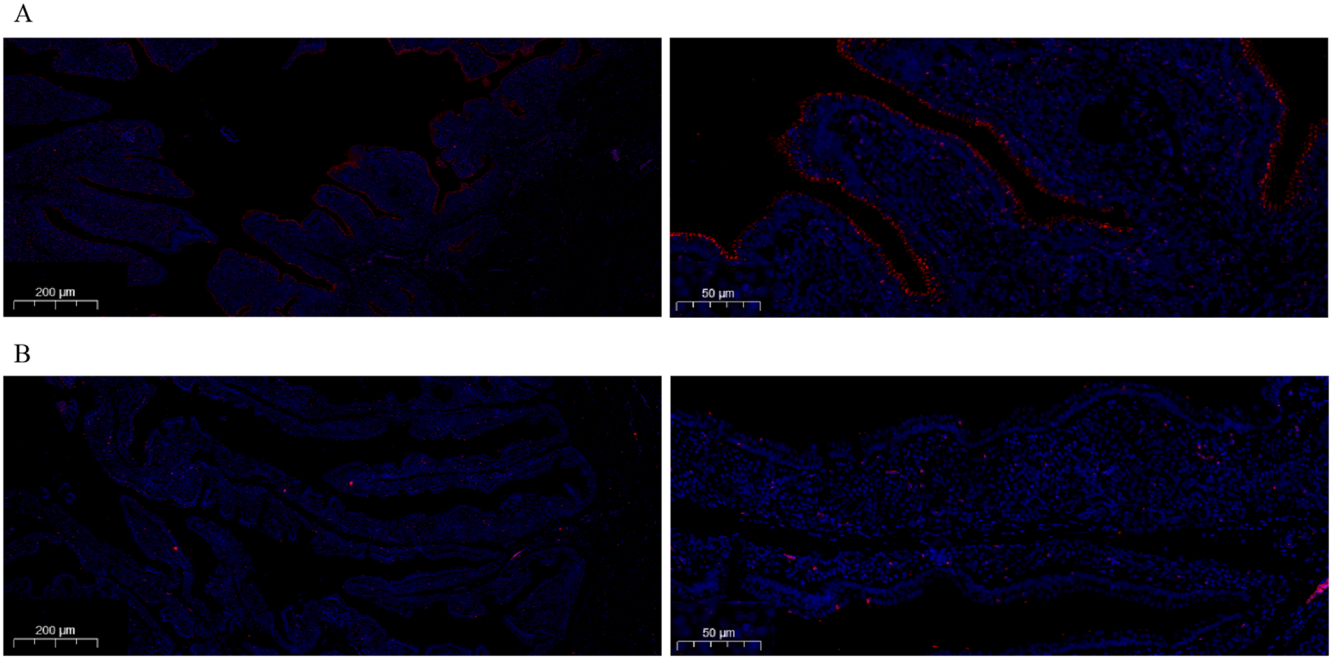

Fig. 5. In situ validation of mRNA expression of *SPP1* in two groups. **A** shows the fluorescence signal of *SPP1* in the control group. **B** shows the fluorescence signal of *SPP1* in the speckled group.

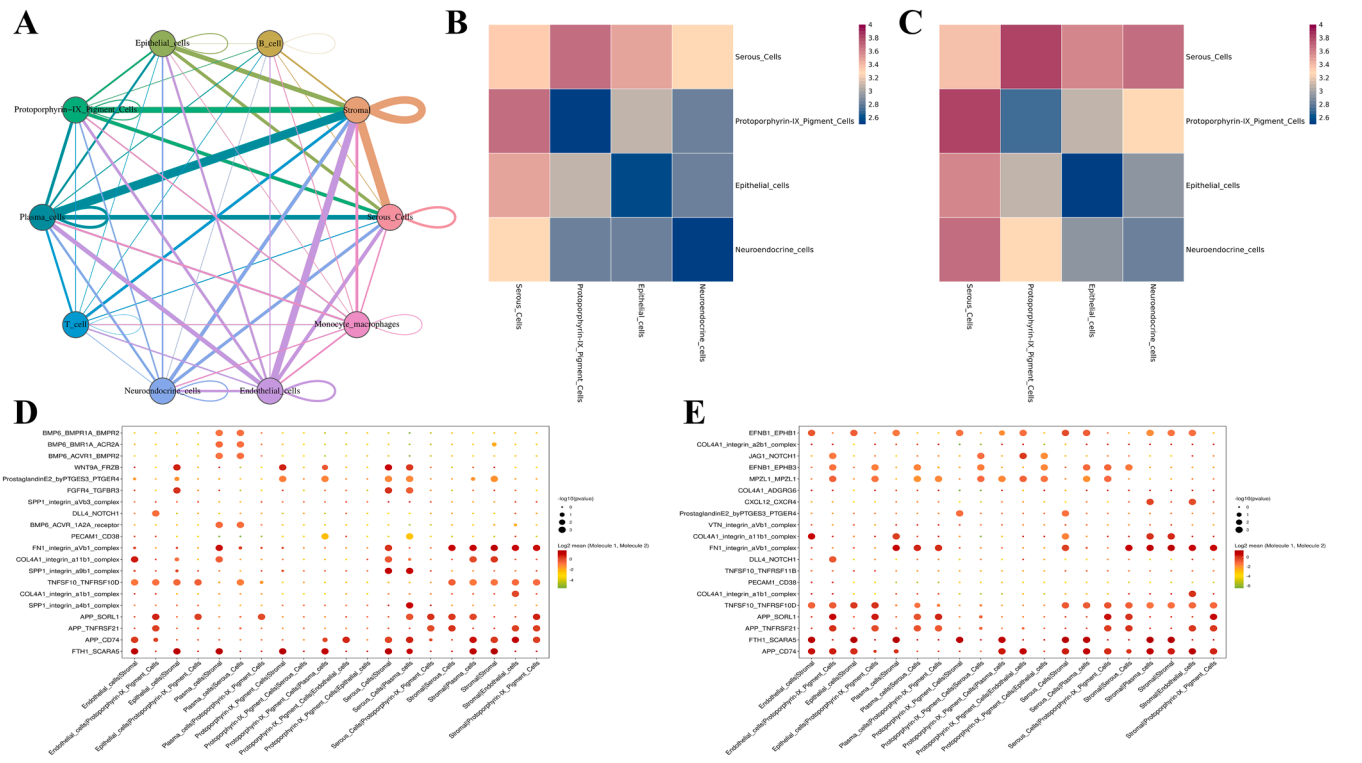

Fig. 6. scRNA-seq reveals cell communication changes in two groups. **A** Overall signaling crosstalk among various cell types. **B** shows the communication strength of cell types in control group. **C** shows communication strength of cell types in speckled group. **D** shows the significant ligand-receptor interactions in control group. **E** shows the significant ligand-receptor pairs in speckled group.

using scRNA-seq, providing insights into this speckled trait. Ten cell types were identified, and their corresponding expression profiles were mapped to the uterus. The proportions of cell subsets and differential expression of cell types between the two groups were compared. These included four types of immune cells, which accounted for 28.5% in the control group and 49.8% in the speckled group, possibly because of the age of the hens. This result indicates that the aged uterus tends to exhibit enhanced barrier defense. We specifically labeled the pigment-synthesizing cells according to the key genes of the protoporphyrin IX pigment synthesis pathway, which also belongs to the epithelial cell type. The proportion of cell types was no significant difference in two groups. This study used three control and three speckled hens, which is a small sample size that limits how broadly the results can be generalized.

The identified marker genes of cell types, which play important roles in eggshell formation. *MEPE* and *SPP1* are marker genes of serous cells, and both were DEGs in two groups. *MEPE* is also known as *OC-116* (ovocleidin 116). OC-116 is the major component of the eggshell matrix, plays an important role in the regulation of calcite growth during eggshell calcification, and is positively correlated with the thickness of the effective layer (Marie et al., 2015). *OC-116* is also expressed in the tibia and mandible of chicken embryos and plays a role in osteogenesis, mineralization, and phosphatemia regulation (Bardet et al., 2010). Meanwhile, multiple signaling pathways such as oxidative phosphorylation, endocytosis were annotated in serous cells, which may be a key cell type in the uterus during eggshell formation.

The epithelial cells are important experimental materials for studying the uterine regulation mechanism of eggshell mineralization. In our result, *OC17* (ovocleidin 17), *EDIL3* (EGF repeats, discoidin domains 3), *TF* (transferrin), and *SAA* (serum amyloid A) have been identified as marker genes of epithelial cells. Furthermore, *OC17* was only upregulated in the serous cells and T cells of the speckled group. *TF* and *SAA* were also upregulated in the epithelial cells of the speckled group. OC17 is an eggshell matrix protein that controls and regulates calcium carbonate deposition in the calcified eggshell layers (Lakshminarayanan et al., 2005; Reyes-Grajeda et al., 2004). Proteomic qualitative analyses of uterine fluid have identified proteins related to mineralization including OC17, and the novel calcium-binding protein-EDIL3 (Marie et al., 2015). We annotated WNT and TGF-beta signaling pathways, which have been reported to play a role in cell proliferation and differentiation (Kahata et al., 2018; Zhao et al., 2021). These two pathways may influence epithelium and play roles in eggshell formation.

In protoporphyrin IX pigment-synthesizing cells, *RARRES1* (retinoic acid receptor responder 1) is a key marker gene, also known as *OCX32* (ovocalyxin-32). This gene was upregulated in B, T, and serous cells of the speckled group. OCX32, an eggshell matrix protein, is expressed at high levels in the uterine and isthmus regions of the oviduct. In the eggshell, OCX32 localizes to the outer palisade layer, vertical crystal layer, and cuticle (Gautron et al., 2001). *OCX32* haplotypes are associated with eggshell quality and are useful markers of eggshell traits (Takahashi et al., 2010).

In the DEGs analysis of the two groups, *SPP1* was highly expressed in all cell types of the control group. *SPP1* is synthesized by granular cells in the uterine surface epithelium (Fernandez et al., 2003). It is secreted into the uterine fluid along with other matrix proteins, where it accumulates in mineralizing eggshells. SPP1 is a highly phosphorylated acidic glycoprotein and influences eggshell structures by regulating crystal growth and morphology (Chien et al., 2008; Panheleux et al., 1999). A lower abundance of SPP1 has been identified in weak eggshells than in strong ones (Sun et al., 2013). Athanasiadou et al. (2018) demonstrated that higher concentrations of SPP1 led to a smaller nanostructure size. Previous research has highlighted the association between *SPP1* expression and abnormalities in corrugated, pimpled, and cracked eggshells (Arazi et al., 2009). In this study, single-cell transcriptomic of uterus-producing speckled eggshells also revealed down-regulation of *SPP1* expression in each uterine cell type.

Cell communication network showed that the interaction signals of speckled group were significantly enhanced compared to the control

group and the shared core ligand-receptor maintained cross cell type communication. The enhanced interaction signals may alter the microenvironment of the uterus, thereby affecting the formation of speckle eggshells. We also identified the altered intercellular communication. Among them, SPP1 interacting with integrin αVβ3, can activate several downstream signaling pathways, such as the PI3K/Akt, NF-κB, and STAT3 pathways, implicated in a variety of physiological and pathophysiological processes (Urtasun et al., 2012). This interaction was only detected in control group. In addition, JAG1-NOTCH1 regulates cell proliferation, differentiation, and apoptosis through the Notch signaling pathway, and maintaining tissue homeostasis (Li et al., 2025). Chemokines play a crucial role in cell migration, which participate in physiological processes such as organizational repair and guidance of immune cells (Rossi et al., 2000). In speckled group, Notch and chemokine signaling pathways were activated. The activation/inhibition of specific signaling may be associated with the formation of speckled eggshell. The single-cell atlas and cell type specific expression-patterns that can guide future functional studies in eggshell formation.

Conclusion

This study demonstrates a single-cell atlas and cellular heterogeneity of chicken uterus in relation to speckled eggs. In total, ten distinct cell types were identified, particularly annotated the protoporphyrin IX pigment-synthesizing cells. The altered cellular communication, activation and inhibition of specific signaling pathways and key genes significantly influenced eggshell speckle traits. Further studies are required to explore how these gene expression patterns vary across different breeds and developmental stages. This study establishes a foundation for targeted improvements in poultry egg production and quality through molecular insights.

Ethics approval

All animal procedures were approved by the Institutional Review Board of the Institutional Animal Care and Use Committee of Shandong Academy of Agricultural Science (protocol code: SAAS-2021-018).

Data availability statement

The datasets analyzed during the current study are available in the Genome Sequence Archive (https://ngdc.cncb.ac.cn/gsub/submit/gsa/) repository under the BioProject no. CRA027347.

CRediT authorship contribution statement

Yan Sun: Writing – original draft, Conceptualization. **Jing Zhang:** Data curation. **Zhongsheng Chen:** Data curation. **Wei Liu:** Formal analysis. **Haixia Han:** Formal analysis. **Dan Hao:** Investigation. **Dapeng Li:** Methodology. **Jie Wang:** Data curation. **Jie Liu:** Supervision. **Qiuxia Lei:** Conceptualization. **Yan Zhou:** Validation. **Dingguo Cao:** Conceptualization. **YunChao Wang:** Resources. **Guiming Li:** Funding acquisition. **Fu Chen:** Project administration. **Fuwei Li:** Writing – review & editing, Funding acquisition.

Disclosures

The authors declare that they have no competing financial interests or personal relationships that could have appeared to influence the work reported in this paper.

Acknowledgements

This research was funded by STI2030-Major Projects (Grant No. 2023ZD0405202), Key R&D Program of Shandong Province, China: Agricultural Breed Project of Shandong Province (Grant No. 2025LZGC048), the Special Fund for China Agricultural Research System program (Grant No. CARS-40-S12), Key R&D Program of Shandong Province, China: Agricultural Breed Project of Shandong Province (Grant No. 2022LZGC013), the Taishan Industry Experts Program (Grant No. TSCX202312057 and No. TSCX202306046), and Key R&D Program of Shandong Province, China: (Grant No. 2024CXPT025).

We are also grateful for bioinformatics support from Xiaoli Meng (LC-Bio Technology co.,ltd.).

Supplementary materials

Supplementary material associated with this article can be found, in the online version, at doi:10.1016/j.psj.2026.106581.

References

Arango, J.A., Settar, P., Arthur, J.A., O'Sullivan, N.P., 2006. Relationship between shell color and incidence of speckles in brown egg lines. In: Proc XIIth European Poultry Conference, pp. 10–14.

Arazi, H., Yoselewitz, I., Malka, Y., Kelner, Y., Genin, O., Pines, M., 2009. Osteopontin and calbindin gene expression in the eggshell gland as related to eggshell abnormalities. Poult. Sci. 88, 647–653.

Athanasiadou, D., Jiang, W., Goldbaum, D., Saleem, A., Basu, K., Pacella, M.S., Böhm, C. F., Chromik, R.R., Hincke, M.T., Rodríguez-Navarro, A.B., Vali, H., Wolf, S.E., Gray, J.J., Bui, K.H., McKee, M.D., 2018. Nanostructure, osteopontin, and mechanical properties of calcitic avian eggshell. Sci. Adv. 4, eaar3219.

Bardet, C., Vincent, C., Lajarille, M.C., Jaffredo, T., Sire, J.Y., 2010. OC-116, the chicken ortholog of mammalian MEPE found in eggshell, is also expressed in bone cells. J. Exp. Zool. B Mol. Dev. Evol. 314, 653–662.

Butler, A., Hoffman, P., Smibert, P., Papalexi, E., Satija, R., 2018. Integrating single-cell transcriptomic data across different conditions, technologies, and species. Nat. Biotechnol. 36, 411–420.

Chen, X., Li, X., Zhong, C., Jiang, X., Wu, G., Li, G., Yan, Y., Yang, N., Sun, C., 2024. Genetic patterns and genome-wide association analysis of eggshell quality traits of egg-type chicken across an extended laying period. Poult. Sci. 103, 103458.

Cheng, X., Fan, C., Ning, Z., 2019. Quality of freckle eggs and its influencing factors. China Poult. 41, 6–9.

Cheng, X., Li, X., Liu, Y., Ma, Y., Zhang, R., Zhang, Y., Fan, C., Qu, L., Ning, Z., 2023a. DNA methylome and transcriptome identified key genes and pathways involved in speckled eggshell formation in aged laying hens. BMC Genom. 24, 31.

Cheng, X., Li, X., Yang, M., Zheng, C., Li, H., Qu, L., Ning, Z., 2023b. Genome-wide association study exploring the genetic architecture of eggshell speckles in laying hens. BMC Genom. 24, 704.

Cheng, X., Ma, Y., Li, X., Liu, Y., Zhang, R., Zhang, Y., Fan, C., Qu, L., Ning, Z., 2023c. Structural characteristics of speckled chicken eggshells and their effect on reproductive performance. Poult. Sci. 102, 102376.

Chien, Y.C., Hincke, M.T., Vali, H., McKee, M.D., 2008. Ultrastructural matrix-mineral relationships in avian eggshell, and effects of osteopontin on calcite growth in vitro. J. Struct. Biol. 163, 84–99.

Choi, H.J., Jung, K.M., Park, K.J., Lee, K.Y., Woo, S.J., Han, J.Y., 2023. Single-cell transcriptome analysis of male chicken germ cells reveals changes in signaling pathway-related gene expression profiles during mitotic arrest. Febs. Open Bio. 13, 833–844.

Duan, G., Liu, W., Han, H., Li, D., Lei, Q., Zhou, Y., Liu, J., Wang, J., Du, Y., Cao, D., Chen, F., Li, F., 2023. Transcriptome and histological analyses on the uterus of freckle egg laying hens. BMC Genom. 24, 738.

Estermann, M.A., Williams, S., Hirst, C.E., Roly, Z.Y., Serralbo, O., Adhikari, D., Powell, D., Major, A.T., Smith, C.A., 2020. Insights into gonadal sex differentiation provided by single-cell transcriptomics in the chicken embryo. Cell Repo. 31, 107491.

Fernandez, M.S., Escobar, C., Lavelin, I., Pines, M., Arias, J.L., 2003. Localization of osteopontin in oviduct tissue and eggshell during different stages of the avian egg laying cycle. J. Struct. Biolo. 143, 171–180.

Gao, L.B., Fu, Y., Guo, Y.T., Zhang, H.J., Qi, G.H., Wang, J., 2025. Proteomic changes in extracellular vesicle and uterine fluid proteins correlated with eggshell quality in aged laying hens. Poult Sci. 104, 105939.

Garcia-Alonso, L., Lorenzi, V., Mazzeo, C.I., Alves-Lopes, J.P., Roberts, K., SanchoSerra, C., 2022. Single-cell roadmap of human gonadal development. Nature 607, 540–547.

Gautron, J., Hincke, M.T., Mann, K., Panheleux, M., Bain, M., McKee, M.D., Solomon, S. E., Nys, Y., 2001. Ovocalyxin-32, a novel chicken eggshell matrix protein. Isolation, amino acid sequencing, cloning, and immunocytochemical localization. J. Biol. Chem. 276, 39243–39252.

Ge, T., Wen, Y., Li, B., Huang, X., Jiang, S., Zhang, E., 2023. Single-cell sequencing reveals the reproductive variations between primiparous and multiparous Hu ewes. J. Anim. Sci. Biotechnol. 14, 144.

Giladi, A., Cohen, M., Medaglia, C., Baran, Y., Li, B., Zada, M., Bost, P., Blecher-Gonen, R., Salame, T.M., Mayer, J.U., David, E., Ronchese, F., Tanay, A., Amit, I., 2020. Dissecting cellular crosstalk by sequencing physically interacting cells. Nat. Biotechnol. 38, 629–637.

Kahata, K., Dadras, M.S., Moustakas, A., 2018. TGF-β family signaling in epithelial differentiation and epithelial-mesenchymal transition. Cold Spring Harb. Perspect Biol. 10, a022194.
Lakshminarayanan, R., Joseph, J.S., Kini, R.M., Valiyaveettil, S., 2005. Structure-function relationship of avian eggshell matrix proteins: a comparative study of two major eggshell matrix proteins, ansocalcin and OC-17. Biomacromolecules 6, 741–751.
Lewis, P.D., Danisman, R., Gous, R.M., 2008. Illuminance, sexual maturation, and early egg production in female broiler breeders. Br. Poult. Sci. 49, 649–653.
Li, J., Xing, S., Zhao, G., Zheng, M., Yang, X., Sun, J., Wen, J., Liu, R., 2020. Identification of diverse cell populations in skeletal muscles and biomarkers for intramuscular fat of chicken by single-cell RNA sequencing. BMC Genomics 21, 752.
Li, X.J., Morgan, C., Li, L., Zhang, W.Y., Chrysostomou, E., Doetzlhofer, A., 2025. The Notch ligand Jagged1 plays a dual role in cochlear hair cell regeneration. Nat Commun 16, 8169.
Marie, P., Labas, V., Brionne, A., Harichaux, G., Hennequet-Antier, C., Rodriguez-Navarro, A.B., Nys, Y., Gautron, J., 2015. Quantitative proteomics provides new insights into chicken eggshell matrix protein functions during the primary events of mineralisation and the active calcification phase. J. Proteomics. 126, 140–154.
Maxwell, M., Söderlund, R., Härtle, S., Wattrang, E., 2024. Single-cell RNA-seq mapping of chicken peripheral blood leukocytes. BMC Genomics 25, 124.
McDavid, A., Finak, G., Chattopadyay, P.K., Dominguez, M., Lamoreaux, L., Ma, S.S., Roederer, M., Gottardo, R., 2013. Data exploration, quality control and testing in single-cell qPCR-based gene expression experiments. Bioinformatics 29, 461–467.
Molnar, A., Maertens, L., Ampe, B., Buyse, J., Kempen, I., Zoons, J., Delezie, E., 2016. Changes in egg quality traits during the last phase of production: is there potential for an extended laying cycle? Br. Poult. Sci. 57, 842–847.
Panheleux, M., Bain, M., Fernandez, M.S., Morales, I., Gautron, J., Arias, J.L., Solomon, S.E., Hincke, M., Nys, Y., 1999. Organic matrix composition and ultrastructure of eggshell: a comparative study. Br. Poult. Sci. 40, 240–252.
Potter, S.S., 2018. Single-cell RNA sequencing for the study of development, physiology and disease. Nat. Rev. Nephrol. 14, 479–492.
Rao, L., Cai, L., Huang, L., 2023. Single-cell dynamics of liver development in postnatal pigs. Sci. Bull. 68, 2583–2597.
Reyes-Grajeda, J.P., Moreno, A., Romero, A., 2004. Crystal structure of ovocleidin-17, a major protein of the calcified Gallus gallus eggshell: implications in the calcite mineral growth pattern. J. Biol. Chem. 279, 40876–40881.
Rossi, D., Zlotnik, A., 2000. The biology of chemokines and their receptors. Annu. Rev. Immunol 18, 217–242.
Samiullah, S., Roberts, J.R., Chousalkar, K., 2015. Eggshell color in brown-egg laying hens - a review. Poult. Sci. 94, 2566–2575.
Sirri, F., Zampiga, M., Berardinelli, A., Meluzzi, A., 2018. Variability and interaction of some egg physical and eggshell quality attributes during the entire laying hen cycle. Poult. Sci. 97, 1818–1823.
Sun, C., Xu, G., Yang, N., 2013. Differential label-free quantitative proteomic analysis of avian eggshell matrix and uterine fluid proteins associated with eggshell mechanical property. Proteomics 13, 3523–3536.
Takahashi, H., Sasaki, O., Nirasawa, K., Furukawa, T., 2010. Association between ovocalyxin-32 gene haplotypes and eggshell quality traits in an F2 intercross between two chicken lines divergently selected for eggshell strength. Anim. Genet. 41, 541–544.
Tian, Y., Sun, P., Liu, W.X., Shan, L.Y., Hu, Y.T., Fan, H.T., Shen, W., Liu, Y.B., Zhou, Y., Zhang, T., 2022. Single-cell RNA sequencing of the Mongolia sheep testis reveals a conserved and divergent transcriptome landscape of mammalian spermatogenesis. FASEB J. 36, e22348.
Trapnell, C., 2015. Defining cell types and states with single-cell genomics. Genome Res 25, 1491–1498.
Underwood, T.J., Sealy, S.G., 2002. Adaptative significance of egg coloration,chapter 19. in Deeming DC Avian Incubation: Behaviour, Environment and Evolution. Oxford University Press, Oxford, UK, pp. 280–298.
Urtasun, R., Lopategi, A., George, J., Leung, T.M., Lu, Y., Wang, X., Ge, X., Fiel, M.I., Nieto, N., 2012. Osteopontin, an oxidant stress sensitive cytokine, up-regulates collagen-I via integrin alpha(V)beta(3) engagement and PI3K/pAkt/NFkappaB signaling. Hepatology 55, 594–608.
Wang, T., Leng, D., Cai, Z., Chen, B., Li, J., Kui, H., Li, D., Li, Z., 2024. Insights into left-right asymmetric development of chicken ovary at the single-cell level. J. Genet. Genomics. 51, 1265–1277.
Wang, Y., Zhao, Y., Chen, S., Chen, X., Zhang, Y., Chen, H., Liao, Y., Zhang, J., Wu, D., Chu, H., Huang, H., Wu, C., Huang, S., Xu, H., Jia, B., Liu, J., Feng, B., Li, Z., Qin, D., Pei, D., Cai, J., 2022. Single cell atlas of developing mouse dental germs reveals populations of CD24+ and Plac8+ odontogenic cells. Sci. Bull. 67, 1154–1169.
Wilson, P.W., Suther, C.S., Bain, M.M., Icken, W., Jones, A., Quinlan-Pluck, F., Olori, V., Gautron, J., Dunn, I.C., 2017. Understanding avian egg cuticle formation in the oviduct: a study of its origin and deposition. Biol. Reprod. 97, 39–49.
Xu, D., Wan, B., Qiu, K., Wang, Y., Zhang, X., Jiao, N., Yan, E., Wu, J., Yu, R., Gao, S., Du, M., Liu, C., Li, M., Fan, G., Yin, J., 2023. Single-cell RNA-sequencing provides insight into skeletal muscle evolution during the selection of muscle characteristics. Adv. Sci. (Weinheim) 10, e2305080.
Zhang, W., Chen, X., Nie, R., Guo, A., Ling, Y., Zhang, B., Zhang, H., 2024. Single-cell transcriptomic analysis reveals regulative mechanisms of follicular selection and atresia in chicken granulosa cells. Food Res. Int. 198, 115368.
Zhao, Y., Meng, K., Yan, Y., Miao, Y., Zhao, X., Wei, Q., Ma, B., 2021. Inhibition of cell proliferation and promotion of acinus-like structure formation from goat mammary epithelial cells via wnt/β-catenin signaling. In. Vitro. Cell. Dev Biol. Anim 57, 676–684.
Zhao, Z.H., Wang, X.Y., Schatten, H., Sun, Q.Y., 2022. Single cell RAN sequencing techniques and applications in research of ovary development and related diseases. Reprod. Toxicol. 107, 97–103.